Strathprints Institutional Repository

Modelling the north-east Atlantic circulation - Implications for the spring invasion of shelf regions by *Calanus finmarchicus.*

Ingo H. Harms, Michael R. Heath, Andrew D. Bryant, Jan O. Backhaus and Dagmar Hainbucher

Harms, I.H., Heath, M.R., Bryant, A.D., Backhaus, J.O. and Hainbucher, D. 2000. Modelling the north-east Atlantic circulation - Implications for the spring invasion of shelf regions by *Calanus finmarchicus.* ICES Journal of Marine Science, 57: 1694-1707 (2000).

The appearance in spring of the copepod *Calanus finmarchicus* in continental shelf waters of the north-eastern Atlantic margin has been hypothesised to be mainly due to invasion from across the continental slope rather than in-situ overwintering. This paper describes the application of a hydrodynamic circulation model and a particle-tracking model to north-east Atlantic waters in order to assess the influence of the flow field and ascent migration parameters on the spring invasion of *C. finmarchicus*.

For hydrodynamic modelling, the Hamburg Shelf Ocean Model (HAMSOM) was applied to the North Atlantic and Nordic Seas and forced with daily mean atmospheric data. Simulated flow fields from HAMSOM serve as forcing functions for a particle-tracking model of the same region. The robustness of the simulated shelf invasion in three target boxes of north-east Atlantic shelf seas was assessed by means of a sensitivity analysis with respect to variations in four key migration parameters: overwintering depth, ascent rate, ascent timing and depth during residence in upper layers.

Our results show that the invasion of the northern North Sea and Norwegian shelf waters is more sensitive to ascent migration parameters than invasion of the Faroese shelf. The main reason for enhanced sensitivity of North Sea invasion is the time and space dependant flow structure in the Faroe-Shetland-Channel. Dense aggregations of overwintering *C. finmarchicus* are found in the Channel, but due to the complex flow field only a proportion of the overwintering stock has the capacity to reach the North Sea.

Ingo H. Harms, Jan O. Backhaus and Dagmar Hainbucher: Institute of Oceanography, University of Hamburg, Troplowitzstrasse 7, 22529 Hamburg, Germany [tel: + 49 (0)40 42838 4206; fax: +49 (0)40 560 5724; E-mail: harms@ifm.uni-hamburg.de]; Michael R. Heath: Marine Laboratory, PO Box 101, Victoria Road, Aberdeen, AB11 9DB, UK; Andrew D. Bryant : Department of Zoology, University of Aberdeen, Tillydrone Avenue, Aberdeen, UK, and Marine Laboratory, PO Box 101, Victoria Road, Aberdeen, AB11 9DB, UK.

Introduction

Productive populations of *C. finmarchicus* are found in the upper layers of both ocean and shelf waters throughout the north-easth Atlantic (Matthews, 1969; Planque and Ibanez, 1997), but aggregations of overwintering copepodites are restricted to layers at 500-2000m depth in the ocean (Heath *et al*., this volume). No open shelf aggregations comparable to those on the Scotian shelf off eastern Canada (Herman et al., 1991*)* or in the Gulf of Maine (Durbin et al., 1995) have been located in the eastern Atlantic. The relationship between continental shelf and the oceanic population has been subject to speculation for many years. Wood (1932) concluded that the summer populations in the northern North Sea were too great to be accounted for by *in-situ* development and reproduction of the population numbers in winter, and that the area must be restocked each year from beyond the shelf edge. This idea was supported by Williams and Lindley (1980), Krause and Martens (1990) and Fransz *et al*. (1991).

Backhaus *et al*. (1994) outlined a hypothesis whereby physical processes at the continental slope might facilitate the transport of overwintered copepodites from depths of 500-1000m, across the shelf edge and into the North Sea each spring. Subsequently, field and modelling studies in the EU-project ICOS (Investigation of *C. finmarchicus* migrations between oceanic and shelf seas off north-west Europe) showed that most of the important features of the Backhaus hypothesis could be supported by field observations and particle-tracking models. Dense aggregations (up to 650 m^{-3}) of overwintering copepodite stage CV were found in the deep overflow water of the Faroe-Shetland Channel and southern Norwegian Sea (Heath and Jónasdóttir, 1999), whilst a tracking model driven by output from a 3-D hydrodynamic model of the region showed that under appropriate meteorological conditions a proportion of these copepodites could be dispersed into the North Sea during their ascent migration in the spring

(Gallego *et al*., 1999*).* Application of year-specific hydrographic and meteorological data for the period 1958-1983 to the tracking model simulated annual invasion indices for the northern North Sea which were highly correlated with abundance of CIV-CVI copepodites measured in the Atlantic inflow to the North Sea by the Continuous Plankton Recorder Surveys (Heath *et al*., 1999*).*

One of the objectives of the EU-project TASC (Trans-Atlantic Study of *C. finmarchicus*) was to extend the concept of the Backhaus hypothesis to other regions of the north-east Atlantic margin. This was achieved by:

- a large-scale mapping of the spatial distribution of overwintering copepodites (*Heath et al.,* this volume),
- development of a hydrodynamic model system to simulate the space-time dynamics of the flow regimes in the region, and
- development of a particle-tracking model to simulate the invasion of a range of shelf sea regions in addition to the North Sea.

The present paper is focussed on the last two points of the above TASC objectives. The main goal of the hydrodynamic modelling was to provide time-dependant flow fields for the particle-tracking model. The north-east Atlantic is characterised by two substantially different flow regimes, the North Atlantic Current system at the surface, which carries warm saline water poleward, and the deep outflow of cold water from the Norwegian Sea into the Atlantic. The latter follows the topography across ridges and through various channels southward. Both current systems are strong and persistent but show variations in speed and transport rates (Harms *et al*., 1999). To account for time-dependant variability of hydrography and currents in the Iceland-Faroe-Shetland area, we decided to produce daily mean hydrodynamic flow

fields of a climatological, so-called 'typical year'. These flow fields were used in a sensitivity study of the particle-tracking model in order to assess the robustness of shelf invasion by *C. finmarchicus* with respect to variations in four key migration parameters: overwintering depth, ascent rate, ascent timing and depth during residence in upper layers.

Materials and Methods

The hydrodynamic model

The current fields in the north-east Atlantic were simulated with the Hamburg Shelf-Ocean Model (HAMSOM) - a three-dimensional, baroclinic level-type model which solves the primitive equations of motion with finite differences on an Arakawa C-grid. The numerical scheme is semi-implicit which allows for economical time steps (Backhaus, 1985). The implicit algorithms are applied for the external gravity waves, for the vertical shear stress and for the vertical diffusion of temperature and salinity. A second order approximation in the time domain is introduced for the Coriolis term and for the baroclinic pressure gradient in the equation of motion. For the pressure field, incompressibility and the hydrostatic equilibrium are assumed, incorporating the Bousinesq approximation.

Vertical, sub-grid scale turbulence is parameterised in HAMSOM by means of a turbulent closure approach, proposed by Kochergin (1987) and later modified by Pohlmann (1996). The scheme is closely related to a Mellor and Yamada (1974) level-2-model where vertical eddy viscosity coefficients depend on stratification and vertical current shear. Convective overturning is parameterised by vertical mixing: an unstable stratification is turned into a neutral state through artificial enlargement of the vertical eddy viscosity coefficient. The

horizontal diffusion of momentum is calculated using a constant, isotropic eddy viscosity coefficient.

HAMSOM includes an Eulerian transport algorithm for temperature and salinity, based on the advection-diffusion equation with an upstream advective flux scheme. Vertical eddy diffusivity coefficients for temperature and salinity are calculated in the same way as the vertical eddy viscosity coefficients. Horizontal eddy diffusion is neglected because of numerical diffusion stemming from the advection scheme.

At open boundaries, the sea level is prescribed. At the sea surface and bottom, kinematic boundary conditions and quadratic stress formulations are applied. The surface heat flux between the ocean and atmosphere is determined by the air and sea surface temperatures, relative humidity, cloud cover and wind speed. These values enter bulk formulae, describing long- and short-wave radiation and sensible and latent heat fluxes (Schrum, 1997).

Hydrodynamic model configuration

Following the example of Hainbucher and Backhaus (1999), a fine resolution (7.5' latitude x 15' longitude) version of HAMSOM for the north-east Atlantic (30°W – 20°E, 56°N – 72°N), nested in a coarse resolution (20' latitude x 40' longitude) model of the whole North Atlantic north of 45°N, was implemented for the TASC project (Figure 1).

The coarse resolution model had 3 layers (0-100 m, 100-600, > 600 m) in the vertical, and was used to prescribe the far-field boundary conditions for the fine resolution model which was focused on the overflow region from the Norwegian Seas. The fine resolution model was resolved with 10 layers: 0-10 m, 10-25 m, 25-50 m, 50-100 m, 100-200 m, 200-400 m, 400-

600 m, 600-1000m, 1000-1500 m, >1500 m. This vertical resolution was adequate to account for the Ekman spiral in the upper layers and the depth horizons of the cold water masses which form the overflow of Norwegian Sea Deep Water into the North Atlantic.

Hydrodynamic model forcing

Topographical data for both models were taken from the ETOPO5 data base (Hirtzler, 1985). The original resolution of 5' x 5' was enlarged to the 7.5' x 15' grid of the fine resolution model and to the 20' x 40' grid of the coarse model. Some modifications were carried out in the Faroe-Bank-Channel and on the Wyville-Thomson Ridge, where the interpolated depths were too small and too large, respectively.

The coarse resolution model was forced with four different wind scenarios, which comprised seasonal means of spatially variable winds taken from the Hellerman data set (Hellerman and Rosenstein, 1983). The initial temperature and salinity distributions were taken from the Levitus (1982) data set. Each seasonal wind scenario was run for three months in a prognostic mode. Sea surface elevations from four seasonal scenarios were interpolated in time and space and prescribed as daily mean values at the open boundaries of the fine resolution model. This was done in order to account for the overall steric height gradient in the northern North Atlantic.

The fine resolution model was forced with climatological daily mean values for wind stress, air pressure, air temperature, relative humidity and cloud cover on the basis of European Centre for Medium Range Weather Forecasting (ECMWF) data. The applied data set was an average over the period 1980-1989. Because time averaging smoothes amplitudes and variability of time series, the averaging procedure treated high and low frequency variability

separately. The low frequency components, averaged over 10 years, were overlaid with the high frequency variability of one particular year. Additionally, the whole averaged data set was adjusted between 31 December and 1 January in order to create a cyclic year of forcing. The result was a so-called 'typical year' that represents on the one hand a repeatable climatological mean situation, but on the other hand included high frequency synoptic variability (eg. storms) with similar properties to realistic forcing.

The fine resolution model was run to a cyclic stationary state (>4 years) using the prognostic mode of simulation. This implied that the three-dimensional advection and diffusion of temperature and salt, sea surface heat fluxes from meteorological forcing and a weak relaxation to seasonal mean Levitus (1982) salinity data. Additionally, seasonal mean values for river run-off were used. For the North Sea and the Norwegian Coast, the values were taken from Damm (1997) and for the river run-off around Iceland, the values were evaluated from Ólafsson et al. (1993) and Rist (1990).

Particle-tracking model

The particle-tracking model involved an Eulerian integration scheme to simulate the horizontal advective trajectories of particles from the spatially and temporally varying flow fields generated by the hydrodynamic model, as previously described by Bryant *et al*. (1998) and *Gallego et al.* (1999). Diffusive contributions to the velocities of particles were not included, so each particle trajectory was essentially deterministic and determined solely by the advective regime. Vertical displacements of particles were prescribed to simulate different ascent migration scenarios for *C. finmarchicus*. Tracking was performed at a fixed 1h time step starting on 1 December, and results were saved at 5d intervals until the end of May in the following year (180 days duration).

The vertical displacement of particles was prescribed by 4 parameters: depth during overwintering (D_1, m); depth during residence in the upper layers (D_2, m); rate of ascent (A, m d^{-1}); and date of onset of the ascent migration (T_A, days from 1 December). Each particle was tracked at its overwintering depth from 1 December until the onset of the ascent migration. Particles were released from a range of depths on a uniform 30km horizontal grid of locations covering an area of the Atlantic and Norwegian Sea extending from 56°N – 69°N and 22°W – 10°E. The abundance of overwintering *C. finmarchicus* in this region was comprehensively sampled over several years by cruises conducted during late November – mid-January (Heath *et al.*, this volume). A composite gridded surface of *C. finmarchicus* abundance (number m^{-2}) was generated from the field data (Heath *et al.*, this volume), and from this the abundance of overwintering animals at each particle release location was estimated by interpolation. Each particle carried this abundance value with it throughout the particle-tracking simulation.

The progress of particle dispersal during a simulation was visualised by aggregating the initial abundance value carried with each particle into 30 km x 30 km cells arranged over the model domain, according to particle locations on a given date. The result was a spatial snapshot of the fate of the initial overwintering stock at a given time.

Particle tracking model strategy

The particle tracking model was used to explore the 4-dimensional parameter space defined by D_1, D_2, A and T_A. Simulations were carried out with 315 different combinations of these parameters covering the ranges D_1 = 600m – 1000m in steps of 100m, this being the range of depths over which the majority of overwintering animals are encountered in the field (Heath and Jónasdóttir, 1999; Heath *et al.*, this volume); D_2 = 5m, 18m and 38m, these being the

mid-depths of each of the three upper levels in the hydrodynamic model; A = 10 m d^{-1}, 15 m d^{-1} and 20 m d^{-1}, these covering the range of estimates from field studies in the region (Heath, 1999); and T_A = 30 December – 28 February in steps of 10 days, this covering the range of possible onset dates estimated from field studies (Heath, 1999). The performance of the particle tracking model with each combination of parameters was evaluated according to the scheme described by Gallego *et al*. (1999). The initial abundance values of all particles which conformed to given spatial and temporal criteria during the tracking period, were summed for each model run. In particular, a set of so called 'target boxes' was specified in the shelf waters (Figure 1), and all particles which entered these boxes within given date ranges were included in the summation process. The summed abundance for a particular run was referred to as the 'invasion index'.

Variations in the invasion index within the 4-dimesional parameter space were visualised by means of grey-scale-shaded diagrams. Each diagram represented the sensitivity of invasion to overwintering depth and ascent timing for fixed values of ascent rate and depth in the upper layers, with the grey-scale representing the value of the invasion index. A set of 9 such diagrams, each being generated from different settings of ascent rate and upper layer depth, portrayed the sensitivity of invasion over the full 4-dimensional parameter space.

Results

Hydrodynamic model results

In presenting results from the hydrodynamic model, we focus here on the flows across the Iceland-Scotland Ridge (Figure 1) because the current speeds, and horizontal and vertical

shears in this area are greatest. Additionally, the Faroe-Shetland Channel is an important overwintering area for *C. finmarchicus.*

In order to visualise structure and variability of the flow field, daily mean current data were averaged to monthly mean values and transport sections were defined across the Faroe-Shetland Channel, across the Faroe-Bank Channel and along the Wyville-Thomson Ridge (Figure 2a, b, c).

The northward transport of Atlantic water masses (T > 3° C, S > 35.1) through a section across the Faroe-Shetland Channel (Figure 2a), ranged between 3 and 7 Sv (1 Sv = 10^6 m^3 s^{-1}), with a mean value of 4.6 Sv, which is in good agreement with estimates by Hansen *et al.* (1998) (4.4 Sv). Direct current measurements (upward-looking ADCP) where carried out between 1994 and 1997 during the Nordic WOCE program. These measurements revealed an average northward flow of 5.1 Sv (Turrell *et al.*, 1999*)* which also compares very well with our computed values. The simulated northward inflow undergoes a significant seasonal variability. Inflow rates were highest in February (7 Sv) and lowest in June (3 Sv). This computed seasonality agrees also well with the above cited WOCE ADCP measurements that give highest inflow in winter and lowest in summer. Turrell *et al.* (1999) stated that the observed summer inflow was approximately half the winter rate which supports our model findings.

The simulated deep outflow through the Faroe-Shetland Channel also showed some seasonal variability. The computed overflow was strongest in June and lowest in Feb./March (Figure 2a). Again, these model result can be compared to ADCP measurements that reached a minimum overflow in autumn and a maximum overflow in spring (Turrell *et al*., 1999). The

average overflow has usually been estimated to range between 1.7 and 1.9 Sv (Hansen *et al*., 1998; Turrell *et al*., 1999). The simulated annual averaged computed overflow was 1.7 Sv.

The computed northward flow across the Wyville-Thomson Ridge (Figure 2b) was significantly higher than through the Faroe-Shetland Channel. The decrease of northward transport from 7.1 to 4.6 Sv was partly due to the Fair Isle current that branches into the North Sea from the North Atlantic current between the Wyville-Thomson Ridge and the Faroe-Shetland section. The threshold values used in Figure 2 for estimating transport rates of different water masses were chosen according to Hansen *et al.* (1998) and other authors cited therein. The chosen values differ between sections due to the enhanced mixing of water masses in the channels and troughs.

The most striking difference between section a and b in Figure 2, however, was the significant seasonality in the northward flow through the Faroe-Shetland Channel, which was not apparent across the Wyville-Thomson Ridge. This can be explained by a seasonally varying surface recirculation cell in the Faroe-Shetland Channel which might bring up to 1.3 Sv (Hansen *et al*., 1998) of Atlantic water masses from around the north of the Faroe Islands. The recirculation cell contributes to the overall northward slope current, particularly in winter, when the cyclonic wind field over the Nordic Seas is stronger than in summer. There was also some Atlantic inflow through the Faroe Bank Channel showing transport rates slightly higher in winter than in summer (Figure 2c). This inflow merged with the northward slope current in the Faroe Shetland Channel and contributed on average 1 Sv.

Figure 3 shows the simulated 10-25m current patterns in January and June which represent the extremes of Atlantic inflow through the Faroe-Shetland. Both flow fields show the

branching of the Fair Isle Current into the North Sea. A recirculation flow from north and south of the Faroe Islands into the Faroe-Shetland Channel was simulated in January, whilst these flows were completely absent in summer. Instead, the June situation shows a weaker northward flow and some southward counter flows in the centre of the Channel.

The time and space variability of the north- and southward flows in the Faroe-Shetland Channel are shown in a series of vertical sections of velocity together with the cross-slope sea surface elevation, corresponding to the barotropic pressure gradient across the Channel. During all months, the core of the northward flow of Atlantic waters can be found on the eastern side of the channel, above the slope. However, the northward flow is much broader and deeper in winter and the current velocities show a maximum during that time.

The intensity of the Atlantic in the Faroe-Shetland Channel, which corresponds to the depicted transport rates in Figure 2a**,** was correlated with the intensity of the cross-slope pressure gradient in Figure 4. One reason for intensified pressure gradients and higher transport rates in winter is the seasonal variance in the meteorological forcing. Frequently occurring low pressure (cyclonic) wind patterns, together with higher wind speeds from south to south-west, drive the surface waters towards the Northwest European Shelf. This results in higher sea levels on the shelf and in stronger northward flows along the continental slope. The far-field forcing from the North Atlantic, which is determined by the large-scale model, contributes to this effect.

The southward overflow close to the bottom of the Faroe-Shetland Channel (Figure 4) showed a clear maximum in spring and summer. Also the vertical extent of southward currents was much larger in spring or summer than in winter. In May and June for example, southward flows extended to the surface as part of a weak recirculation within the Faroe-Shetland

Channel (Figure 3). Although southward currents decrease in winter, the overflow close to the bottom was persistent throughout the year.

Verification of the simulated seasonally varying vertical flow structure is difficult due to the climatological character of the model results and a lack of long-term and high-resolution current measurements. However, observed mean velocity profiles (Turrell *et al.*, 1999) suggest that the general structure is well reproduced by the model. It can be concluded that observed seasonal variations in the through-flow are not only caused by the flow intensity but also by variations in the vertical structure of the along-channel flow field, as the model suggest.

Due to the seasonal variability of the flow structure, a striking difference occurs in mid-depths in the Faroe-Shetland Channel. An example of this seasonal variability is given in Figure 5 which shows monthly mean horizontal flow fields between 400 and 600 m depth (layer 7), for January and June. Whereas in January northward flows are dominating, in June southward flows prevail, blocking the Atlantic inflow in this depth horizon. This figure suggests a seasonally dependant vertical displacement of the boundary layer between northward inflow and southward overflow in the Faroe-Shetland Channel.

Particle tracking model results

The distribution of initial (overwintering) abundance values for each particle on 1 December, interpolated from the field data presented by Heath *et al*. (this volume), shows that particles

originating from south of the Iceland-Scotland Ridge carry consistently low values ($<10^4$ m^{-2}), whilst those from north of the Ridge all carry higher values. Particularly high values of overwintering abundance ($>2.5 \times 10^4$) were attributable to particles originating in the Faroe-Shetland Channel and along the continental slope west of Norway.

An example of the progressive dispersal of the overwintering abundance for a particular combination of vertical displacement parameters is shown in Figure 6. This particular scenario involved transport at an overwintering depth of 900m between 1 December and 10 January, followed by ascent to 5m depth at a rate of 20 m d^{-1}. The initial peak abundance in the Faroe-Shetland Channel and southern Norwegian Sea was transported southwest through the Faroe Bank Channel during the initial period, but then dispersed north-eastwards during the ascent phase. By the end of the run, components of the initial overwintering stock were located in the shelf waters of the northern North Sea, western Norway, Faroe and south of Iceland. Particles entered the northern North Sea by both the Fair Isle Channel and along the western side of the Norwegian Trench. Particles entering by the latter route had high initial weighting and originated mainly from the Faroe Shetland Channel, whilst those entereing through the Fair Isle route originated in the open northeast Atlantic. Particles entered the Norwegian shelf waters by a narrow corridor off Trondheim at around 63EN and around the north of the Lofoten Islands. Some particles were carried out of the northeast corner of the model domain in the direction of the Barents Sea.

The D_1 x T_A parameter space represented by each of the grey-shaded sensitivity diagrams represented a gradient of increasing residence time in the deep overflow circulation regime around the Iceland-Scotland Ridge (highest values towards the bottom right of each diagram). Thus scenarios involving late ascent from deep overwintering depths implied greater influence of the deep circulation on the dispersal trajectories of the particles. The invasion

index results for the North Sea (Figure 7) showed that the transfer of overwintering abundance into the northern North Sea was favoured by minimising residence in the deep circulation regime (i.e. shallow overwintering and early ascent), and also by rapid ascent to shallow depths in the upper layers. Few particles entered the North Sea under a scenario of slow ascent (10m d^{-1}) with upper layer residence at 38m.

Scrutiny of the origins of the particles entering the North Sea target box indicated that a high proportion came from south of the Iceland-Scotland Ridge and carried low overwintering abundance values. The hypothesis of Backhaus *et al*. (1994), reinforced by the modelling and field observations of Gallego *et al*. (1999), Heath *et al*. (1999) and Madden *et a*l. (1999), is that the northern North Sea *C. finmarchicus* production is sustained by invasion from overwintering aggregations in the Faroe-Shetland Channel (Heath and Jónasdóttir, 1999). To isolate the contribution of particles originating in the Faroe-Shetland Channel to the North Sea invasion index, the index summation was restricted to particles carrying an initial abundance $>10^4$ m^{-2}. The results (Figure 8) showed that invasion by particles originating from north of the Iceland-Scotland Ridge on 1 December was restricted to a narrow range of parameters, but the underlying pattern was essentially similar in that combinations which minimised the time spent in the deep circulation regime promoted invasion of the North Sea.

Invasion of the Norwegian shelf was less sensitive to wintering depth and ascent timing than invasion of the North Sea, as indicated by the fact that there was less contrast within the individual panels of Figure 9 than Figure 7. However, the sensitivity with respect to ascent rate and depth in the surface waters was similar in both areas since the contrast between panels was similar in both cases. As for the North Sea, rapid ascent from overwintering at 600m to shallow depths in the surface layers, promoted invasion of the Norwegian shelf region.

Invasion of both the northern and southern Faroese shelf waters was less sensitive to all of the parameters describing vertical displacement behaviour than invasion of the North Sea or Norwegian shelf (Figure 10 and 11). Invasion of the northern Faroese shelf was more sensitive than the southern shelf including Faroe Bank, but in both cases, the weakest invasion resulted from the slowest ascent rates from the deepest overwintering depths and with the latest ascent timings.

Discussion

Our particle-tracking simulations robustly predicted a spring invasion of the Faroes, Norwegian and northern North Sea shelf seas from known overwintering aggregation of *C. finmarchicus* in oceanic waters. Variations in the magnitudes of invasions of the Faroe and Norwegian shelf were relatively small in the context of the uncertainty in ascent migration parameters. However, this uncertainty is potentially very significant for interpreting invasion of the northern North Sea.

The invasion of the North Sea from the important overwintering aggregations in the Faroe-Shetland Channel was sensitive to the overwintering depth and the ascent rate and timing assumed in the model. This means that only a proportion of the overwintering stock has the capability to reach the North Sea. In particular, this capability pertains to the fraction resident between 700 and 900m during the winter, and which reaches the 10-25m depth level in spring. In fact, this envelope of overwintering depth encompasses the majority (>66%) of the stock in the Faroe-Shetland Channel in December (Heath, 1999), so the apparent sensitivity of

the model is not inconsistent with the observation that copepodites do enter the northern North Sea from across the north-western shelf edge.

The background to the enhanced sensitivity of the simulated North Sea invasion lies in the vertical structure of currents in the Faroe-Shetland Channel, in particular the interaction between the northward Atlantic inflow in the upper layers and the southward overflow in the bottom layers (>600 m). A direct pathway for particles invading the North Sea from the north-east Atlantic is formed by the Fair Isle Current that branches between the Orkney and Shetland Islands from the North Atlantic / Shelf Edge Current. A second pathway farther north is formed by the North Sea recirculation that branches north of the Shetland Islands. Both currents are surface flows that extend through the upper 100 - 200 m. However, overwintering *C. finmarchicus* in the Faroe-Shetland Channel reside at more than 600 m depth, within the deep southward overflow. In order to invade the North Sea, particles must ascent to the upper layers in the right locations for entrainment in one or other of the cross-shelf flows forming the invasion routes. Tracking scenarios involving late ascent from deep overwintering depths imply greater influence of the deep circulation on the dispersal trajectories. In these scenarios, particles remained too long in deep overflow and were transported through the Faroe-Shetland and Faroe-Bank Channels, and along the south face of the Iceland-Scotland Ridge from where the liklihood of subsequent dispersal into the North Sea was significantly reduced.

Another reason for greater sensitivity of the North Sea invasion was the time-dependant variability of the simulated circulation in the Faroe-Shetland-Channel. North-flowing upper layer currents were strongest in winter and weakest in summer, whilst the reverse was the case for the deep south-flowing currents. At the same time, the interface between northward inflow and southward overflow became progressively shallower during spring. This seasonal

pattern of variability had the potential to generate an interaction between overwintering depth, ascent rate and timing and the invasion rate of the North Sea.

Invasion of the Faroes and Norwegian shelves was less sensitive to the wintering depth and ascent timing parameters used in the particle-tracking model than for the North Sea. This must indicate that these regions are accessible to a greater proportion of the overwintering stock, and that variations in the circulation regime and hence particle advection play a lesser role. As a result, variation in invasion of these regions should be less than for the North Sea, and the results may suggest that the North Sea is a more marginal area for colonisation by *C. finmarchicus* than the Faroese and Norwegian shelves. Detailed long-term (>30 years) monitoring data from Faroe and Norway are not available to the same extent as in the North Sea. However, indications from Continuous Plankton Recorder data are that these areas have not exhibited the long-term decline in *C. finmarchicus* abundance that has been detected in the northern North Sea (Beare and McKenzie, 1999; Fromentin and Planque, 1996).

In conclusion, our results indicate that simulating the spatio-temporal dynamics of *C. finmarchicus* requires attention not only to representations of hydrodynamics, but also the resolution of variability in overwintering and vertical migration parameters.

Acknowledgments

This study was supported by EU-TASC contract MAS3-CT95-0039. The particle-tracking model was developed from code written by J. Mardaljevic under EU-ICOS contract MAS2-CT94-0085.

References

Backhaus J.O. 1985. A three-Dimensional Model for the Simulation of Shelf Sea Dynamics. Deutsche Hydrographische Zeitung 38: 165-187

Backhaus J.O., Harms, I.H., Krause, M. and Heath, M.R. 1994. An hypothesis concerning the space-time succession of *Calanus finmarchicus* in the northern North Sea. ICES Journal of Marine Science 51: 169-180.

Beare D.J. and McKenzie, E. 1999. The multinomial logit model: a new tool for exploring Continuous Plankton Recorder data. Fisheries Oceanography 8 (Suppl. 1): 126-137.

Bryant A.D., Hainbucher, D. and Heath, M.R. 1998. Basin-scale advection and population persistence of *Calanus finmarchicus*. Fisheries Oceanography 7: 235-244.

Damm P.E. 1997. Die saisonale Salzgehalts- und Frischwasserverteilung in der Nordsee und ihre Bilanzierung. Berichte aus dem Zentrum fuer Meeres- und Klimaforschung, 28, Reihe B: 259 pp

Durbin E.G., Gilman, S.L., Campbell, R.G. and Durbin, A.G. 1995. Abundance, biomass, vertical migration and estimated development rate of the copepod *Calanus finmarchicus* in the southern Gulf of Maine during late spring. Continental Shelf Research 15: 571-591.

Fransz H.G., Colebrook, J.M., Gamble, J.C. and Krause, M. 1991. The zooplankton of the North Sea. Netherlands Journal of Sea Research 28: 1-52.

Gallego A., Mardaljevic, J., Heath, M.R., Hainbucher, D. and Slagstad, D. 1999. A model of the spring migration into the North Sea by *Calanus finmarchicus* overwintering off the Scottish continental shelf. Fisheries Oceanography 8 (Suppl. 1): 107-125.

Fromentin J.-M. and Planque, B. 1996. *Calanus* and environment in the eastern North Atlantic. (2) Role of the North Atlantic Oscillation on *Calanus finamrchicus* and *Calanus helgolandicus*. Marine Ecology Progress Series 134: 111-118.

Hainbucher D. and Backhaus, J.O. 1999. Circulation of the eastern North Atlantic and northwest European continental shelf - a hydrodynamic model study. Fisheries Oceanography 8 (Suppl. 1): 1-12.

Hansen B., Østerhus, S., Dooley, H.D., Gould, W.J. and Rickards, L.J. 1998. North Atlantic - Norwegian Sea Exchange - The ICES NANSEN project. ICES Cooperative Research Report, No. 225: 3-82.

Harms I.H., Backhaus, J.O. and Hainbucher, D. 1999. Modelling the seasonal variability of circulation and hydrography in the Iceland-Faroe-Shetland overflow area. ICES CM 1999/L:10, 7pp

Heath M.R. 1999. The ascent migration of *Calanus finmarchicus* from overwintering depths in the Faroe-Shetland Channel. Fisheries Oceanography 8 (Suppl. 1): 84-99.

Heath M.R., Backhaus, J.O., Richardson, K., McKenzie, E., Slagstad, D., Beare, D., Dunn, J., Fraser, J.G., Gallego, A., Hainbucher, D.A., Hay, S.J., Jónasdóttir, S.H., Madden, H., Mardaljevic, J. and Schacht, A. 1999. Climate fluctuations and the spring invasion of the North Sea by *Calanus finmarchicus*. Fisheries Oceanography 8 (Suppl. 1): 163-176.

Heath M.R., Fraser, J.G., Gislason, A., Hay, S.J., Jonasdóttir, S.H. and Richardson, K. Winter distribution of *Calanus finmarchicus* in the northeast Atlantic. ICES Journal of Marine Science, this volume.

Heath M.R. and Jónasdóttir, S.H. 1999. Distribution and abundance of *overwintering Calanus finmarchicus* in the Faroe-Shetland Channel. Fisheries Oceanography 8 (Suppl. 1): 40-60.

Hellerman, S. and Rosenstein, M. 1983. Normal monthly wind stress over the world ocean with error estimates. Journal of Physical Oceanography, 1983, Vol. 13

Herman A.W., Sameoto, D., Shunnian, C., Mitchell, M.R., Petrie, B. and Cochrane, N. 1991. Sources of zooplankton on the Nova Scotia shelf and their aggregations within deep shelf basins. Continental Shelf Research 11: 211-238.

Hirtzler J.D. (ed.) 1985. Relief of the surface of the earth. MGG-2, National Geographic Data Center, Boulder, Colorado, USA.

Kochergin V.P. 1987. Three-dimensional prognostic models. in: Three-dimensional coastal ocean models (ed. N. Heaps); AGU: Coastal and Estuarine Science 4: 201-208.

Krause M. and Martens, P. 1990. Distribution patterns of mesozooplankton biomass in the North Sea. Helgolaender wissenschaftliche Meeresuntersuchungen 44: 295-327.

Levitus S. 1982. Climatological atlas of the world ocean. NOAA Prof. Pap., 13: 173p

Madden H., Beare, D., Heath, M.R., Fraser, J.G. and Gallego, A. 1999. The spring/early summer distribution of *Calanus* sp. in the northern North Sea and adjacent areas. Fisheries Oceanography 8 (Suppl. 1): 138-152.

Matthews J.B.L. 1969. Continous plankton records: the geographical and seasonal distribution of *Calanus finmarchicus* s.l. in the North Atlantic. Bull. Mar. Ecol. 6: 251-273

Mellor G.L. and Yamada, T. 1974. A hierachy of turbulence closure models for planetary boundary layers. Journal of Atmospheric Science, 31: 1791 - 1806.

Ólafsson J., Johannesson, G. and Stefánsson, G. 1993. Recruitment of Icelandic cod in relation to spawning stock biomass and environmental factors. International Council for the Exploration of the Sea 1993 / CCC Symposium / No. 37

Planque B. and Ibanez, F. 1997. Long-term time-series in *Calanus finmarchicus* abundance - a question of space? Oceanologica Acta 20: 159-164.

Pohlmann T. 1996. Calculating the annual cycle of the vertical eddy viscosity in the North Sea with a three-dimensional baroclinic shelf sea circulation model. Continental Shelf Research, Vol. 16, No. 2: 147-161.

Rist S. 1990. Vatns Er Thorf. Bókaútgáfa Menningarsjóds, Reykjavik

Schrum C. 1997. Thermohaline stratification and instabilities at tidal mixing fronts: results of an eddy resolving model for the German Bight. Continental Shelf Research, Vol. 17, No. 6: 689-716

Turrell W.R., Hansen, B. Osterhus, S. Hughes, S. Ewart, K. and Hamilton, J. 1999. Direct observations of inflow to the Nordic Seas through the Faroe-Shetland Channel 1994-1997. ICES CM 1999/L:01, pp 15.

Williams R. and Lindley, J.A. 1980. Plankton of the Fladen Ground during FLEX-76. III. Vertical distribution, population dynamics and production of *Calanus finmarchicus*. (Crustacea: Copepoda). Marine Biology 60: 47-56.

Wood H. 1932. The natural history of the herring in Scottish waters. The Buckland Lectures, third series for 1932. Aberdeen: Fishing News: 36 pp.

Figures

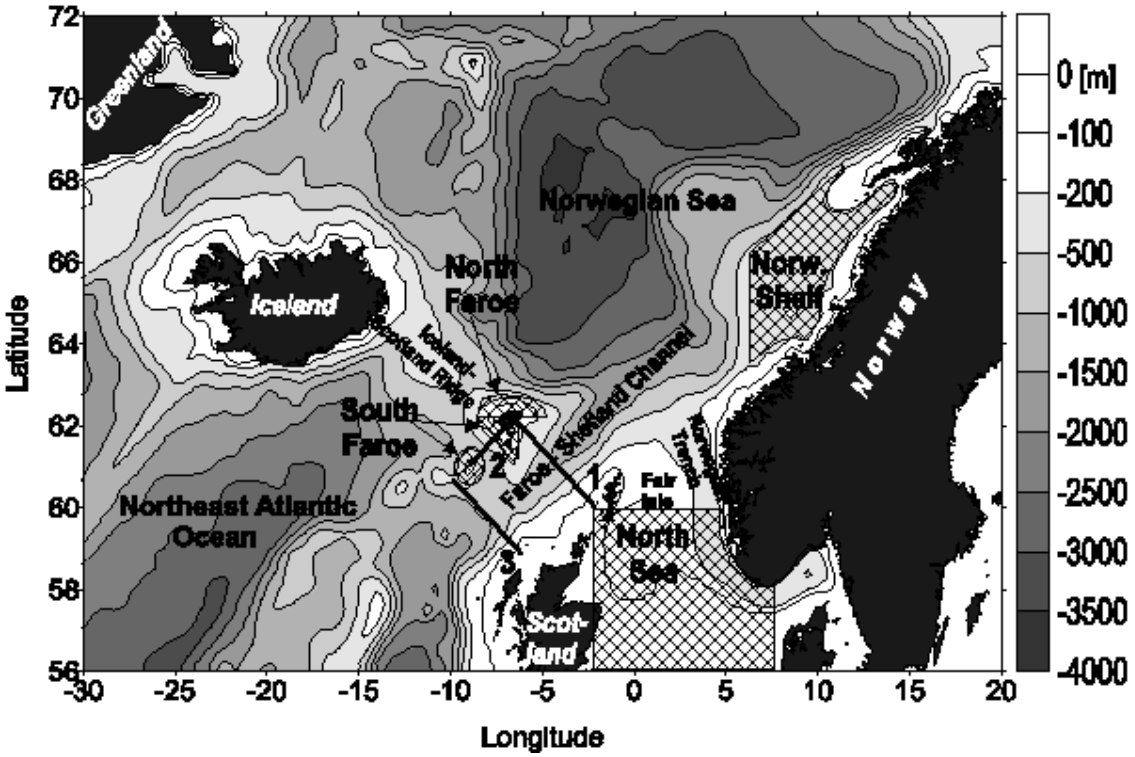

Figure 1: Small scale TASC model domain and topography. Lines denote transport sections: 1=Faroe-Shetland Channel, 2=Faroe Bank Channel, 3=Wyville-Thomson Ridge. Hatched areas denote the shelf sea target boxes North Sea, North Faroe, South Faroe and Outer Norwegian Shelf, used for analysis of particle-tracking results.

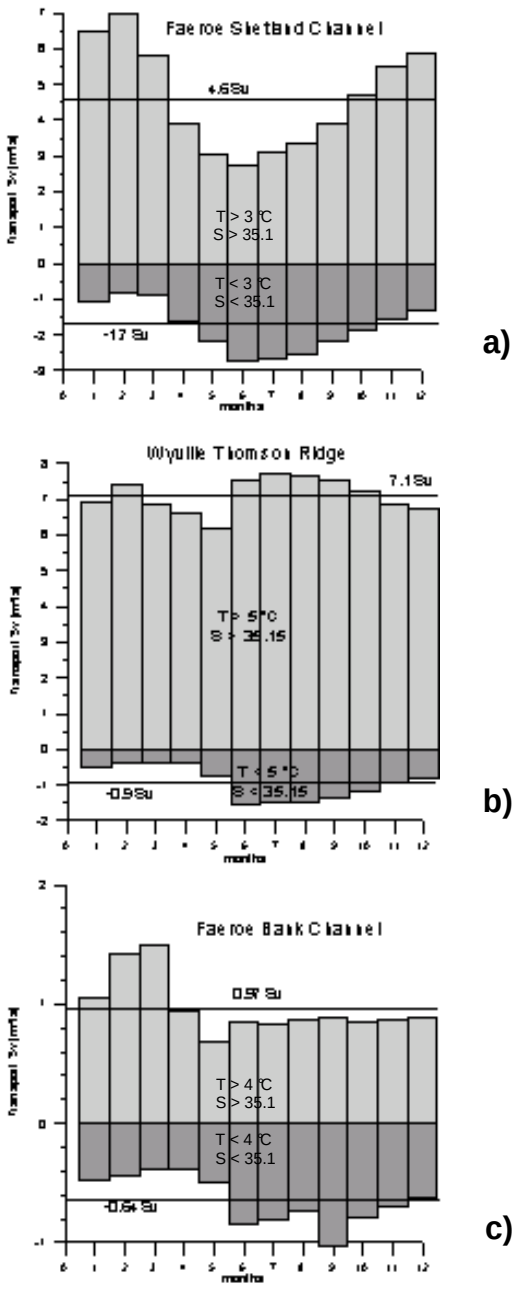

Figure 2: Simulated transport rates in the Faroe-Shetland Channel (a), across the Wyville-Thomson Ridge (b) and in the Faroe Bank Channel (c). The figure shows monthly mean values of the cyclic climatological year. Positive transport rates are northward (Atlantic waters), negative values are southward (overflow).

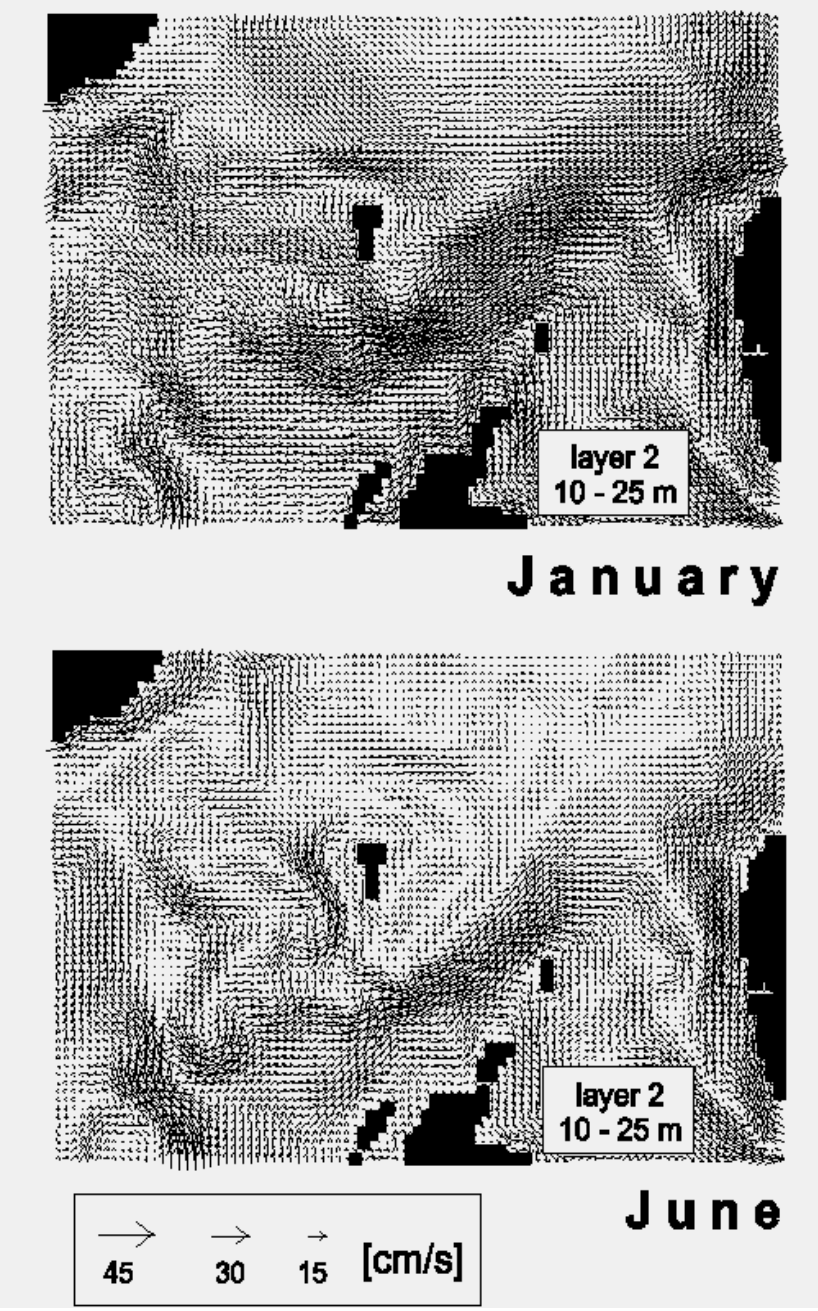

Figure 3: Simulated flows in the 2. layer (10 - 25 m) in the overflow region. Monthly mean values for January (upper panel) and June (lower panel) are depicted.

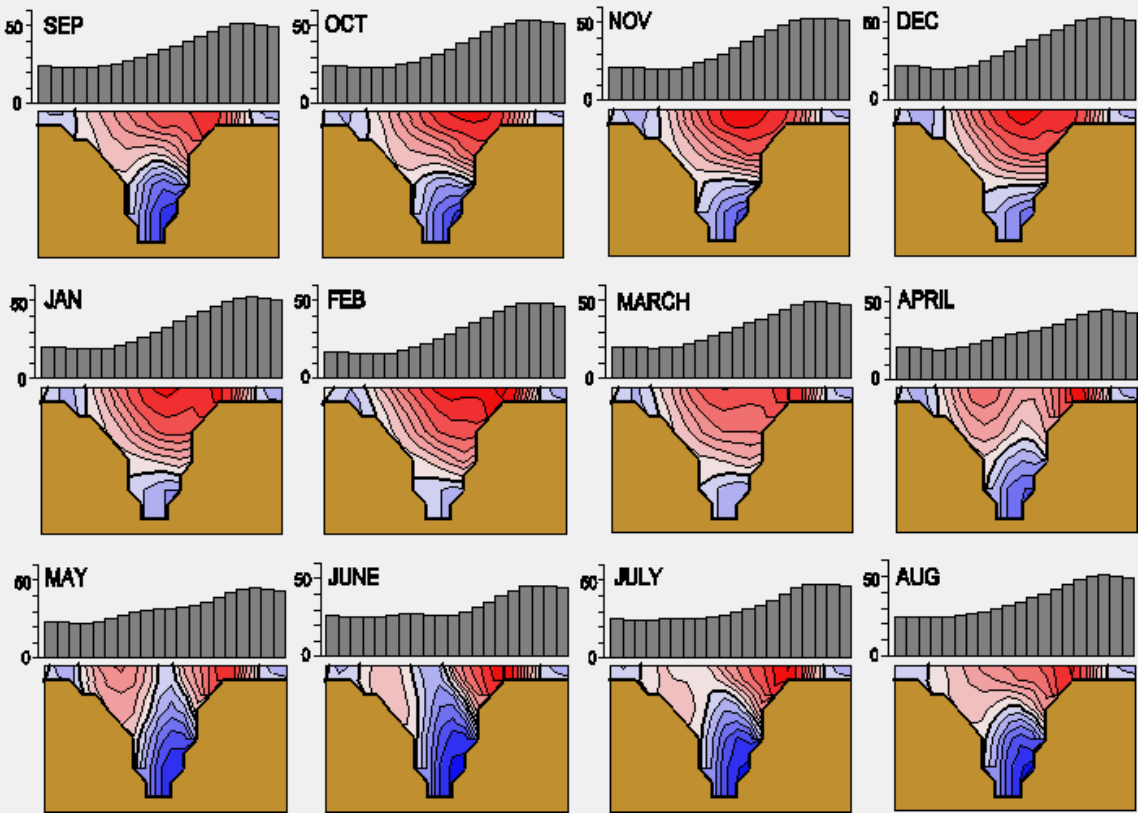

Figure 4: Velocity section (lower panels [cm/s]) and sea surface elevations (upper panels [cm]) across the Faroe-Shetland Channel. The figure shows simulated monthly mean values of the climatological cyclic year. Orientation is northward: left side = Faroe Islands, right side = Shetland Islands. Positive (northward) flow is shaded, negative (southward) flow is hatched. Contour interval 2 cm/s, thick line = 0.

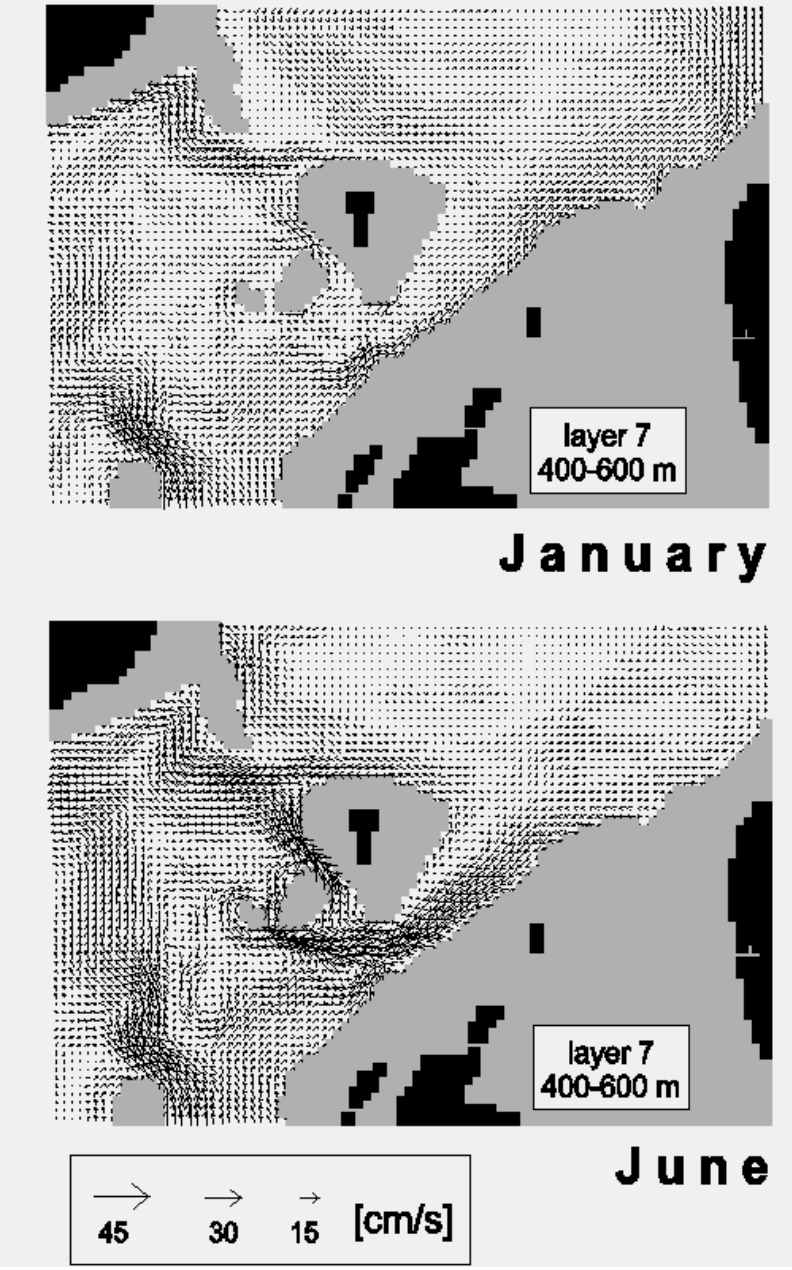

Figure 5: Simulated flows in the 7. layer (400-600 m) in the overflow region. Monthly mean values for January (upper panel) and June (lower panel) are depicted.

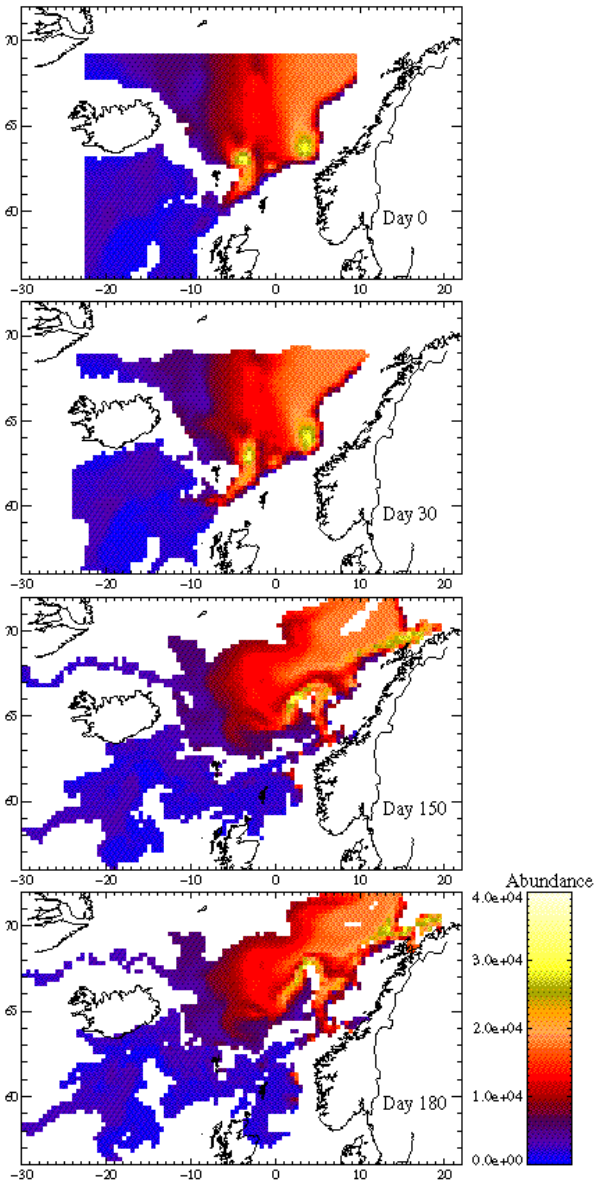

Figure 6: Example of the progressive dispersal of the winter abundance distribution in the particle tracking model. Initial (1 December, day 0) abundance values (m^{-2}) of particles were aggregated into 30km grid cells and displayed as colour shaded values. In this example, particles were held at a depth of 700m from 1 December to 20 January (day 52) and then ascended to 18m depth at a rate of 20 m d^{-1}. The resulting distributions of particle abundance values (m^{-2}), aggregated over 30km grid cells, are shown for day 30 (29 December), day 150 (28 April) and day 180 (28 May).

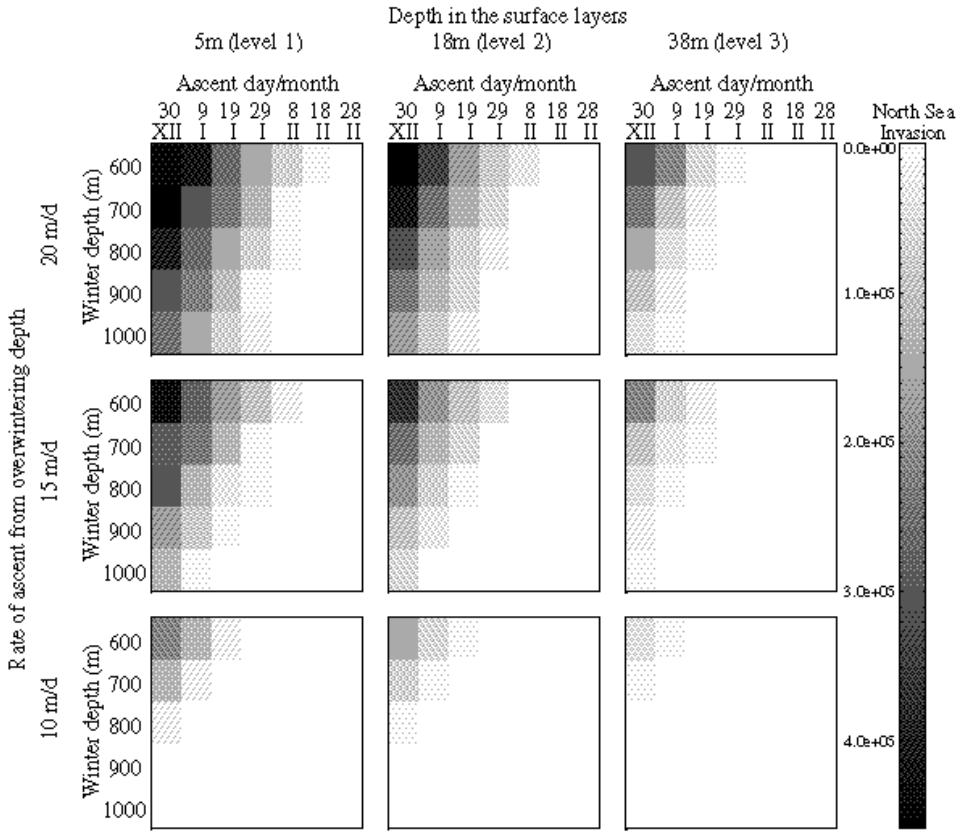

Figure 7: Sensitivity of North Sea invasion to variations in winter depth and ascent timing, and combinations of ascent rate (10, 15 or 20 m d^{-1}) and depth in the surface layers (hydrodynamic model levels 1, 2 or 3). Each individual panel represents the sensitivity to ascent timing (x-axis) and winter depth (y-axis), with the grey-scale representing the magnitude of invasion into the North Sea target box for a given combination of ascent rate and depth in the surface layers. All panels in the same row were derived using the same ascent rate, and all panels in the same column with the same depth in the surface layers. All particles released in the model domain which entered the North Sea were included in the calculation of the invasion index.

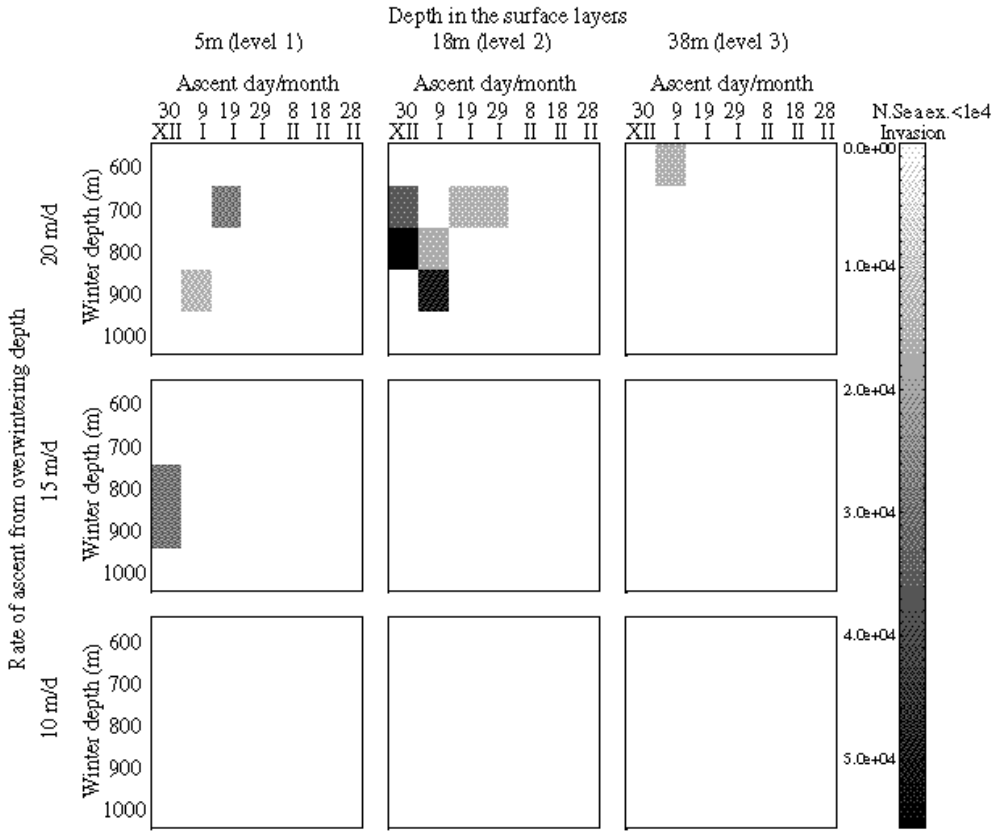

Figure 8: Sensitivity of North Sea invasion to variations in winter depth and ascent timing, and combinations of ascent rate (10, 15 or 20 m d^{-1}) and depth in the surface layers (hydrodynamic model levels 1, 2 or 3), but excluding particles with initial (winter) abundance value $<10^4$ m^{-2}. Organisation of shaded panels as in Figure 7.

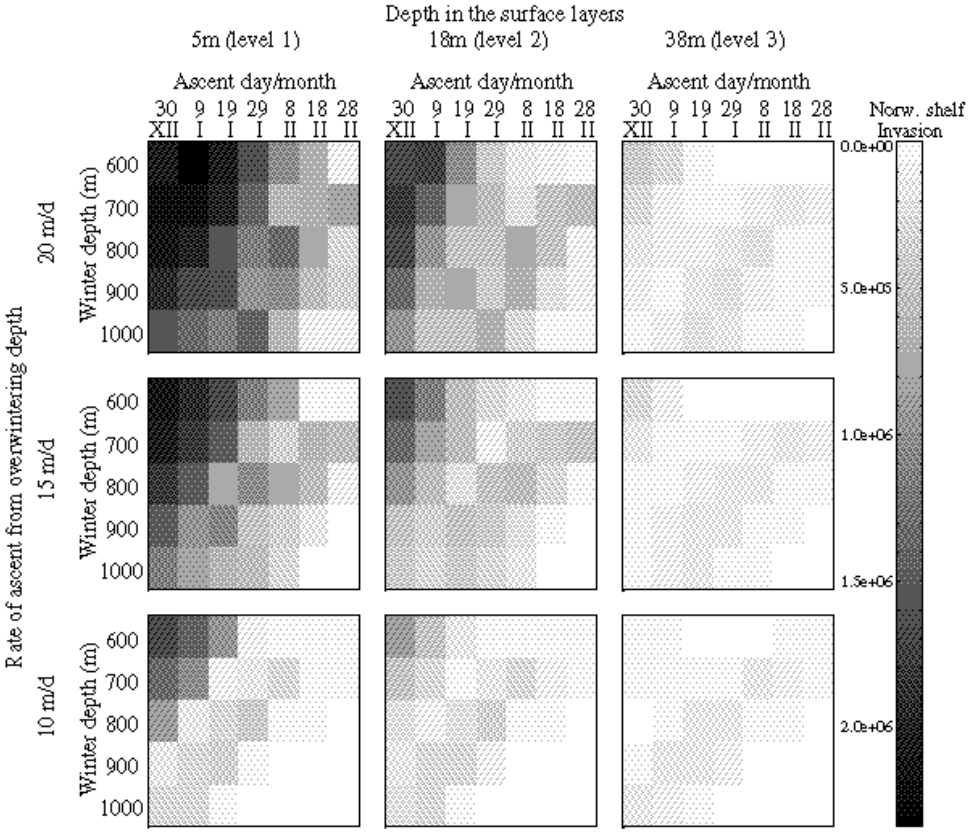

Figure 9: Sensitivity of Norwegian shelf invasion to variations in winter depth and ascent timing, and combinations of ascent rate (10, 15 or 20 m d^{-1}) and depth in the surface layers (hydrodynamic model levels 1, 2 or 3). Organisation of shaded panels as in Figure 7.

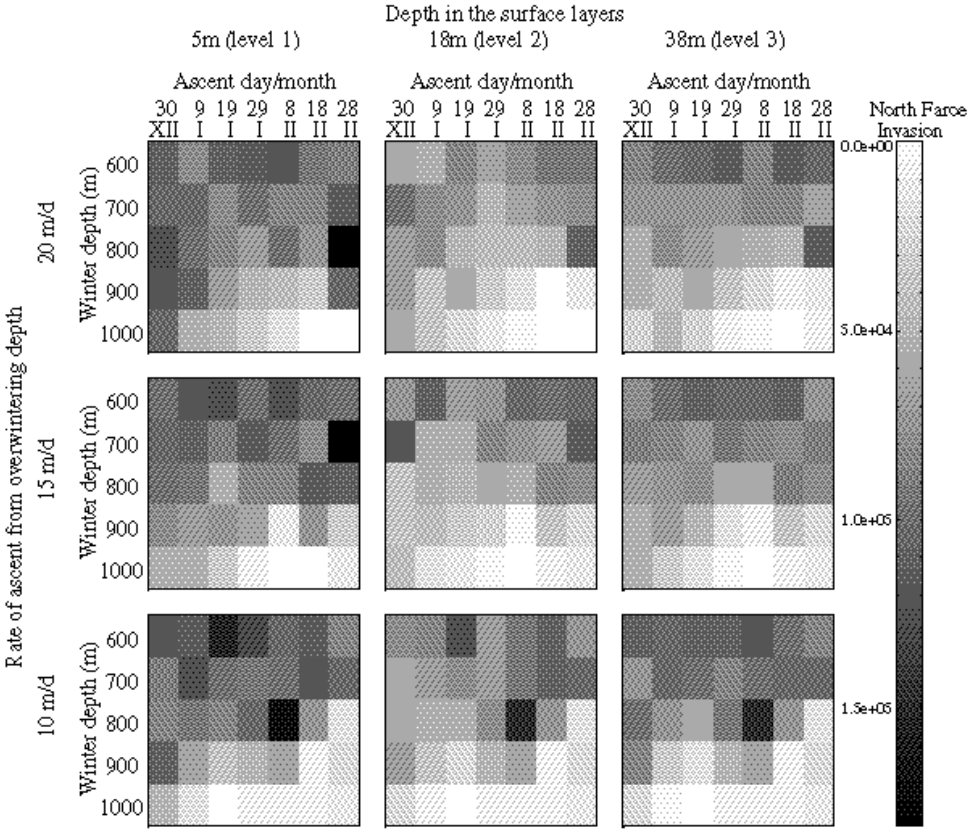

Figure 10: Sensitivity of the northern Faroe shelf invasion to variations in winter depth and ascent timing, and combinations of ascent rate (10, 15 or 20 m d^{-1}) and depth in the surface layers (hydrodynamic model levels 1, 2 or 3). Organisation of shaded panels as in Figure 7.

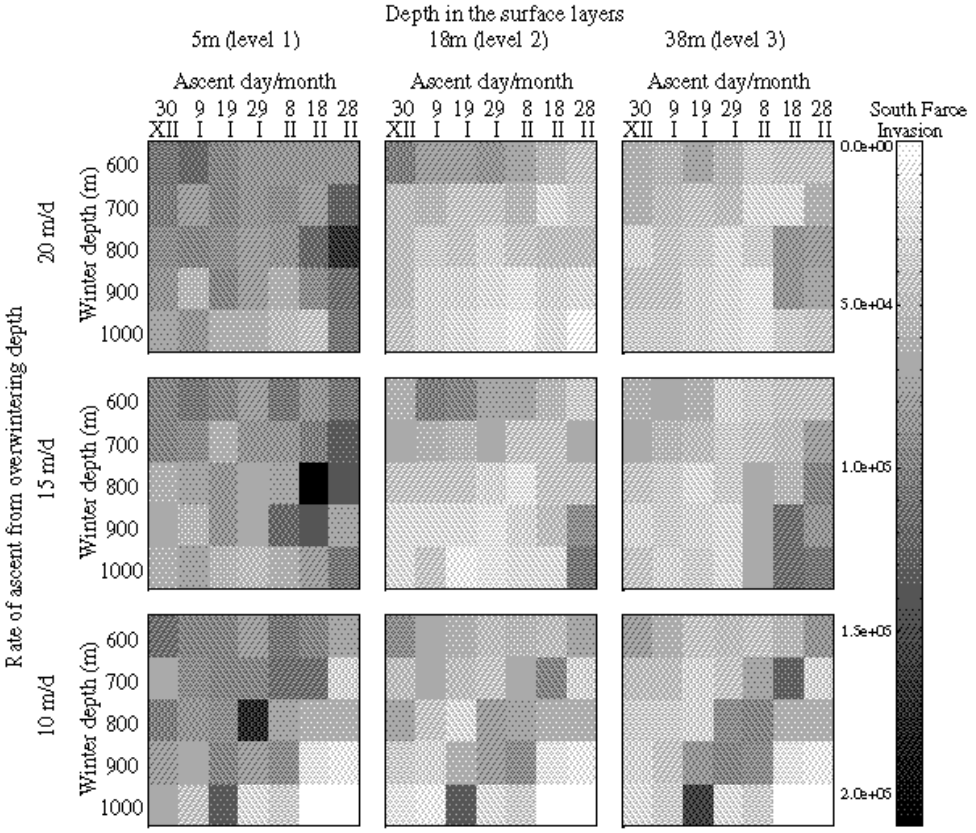

Figure 11: Sensitivity of the southern Faroe shelf invasion to variations in winter depth and ascent timing, and combinations of ascent rate (10, 15 or 20 m d^{-1}) and depth in the surface layers (hydrodynamic model levels 1, 2 or 3). Organisation of shaded panels as in Figure 7.